Electric Birefringence Measurements in Aqueous Polyelectrolyte Solutions

U. Krämer and H. Hoffmann*

Lehrstuhl für Physikalische Chemie I der Universität Bayreuth, Postfach 101251, D-8580 Bayreuth, Germany

Received January 17, 1990; Revised Manuscript Received April 19, 1990

ABSTRACT: Aqueous solutions of poly(sodium *p*-styrenesulfonate) with molecular weights 100 000, 400 000, and 1 200 000 were examined by the transient and dynamic electric birefringence method. On the basis of the results it is demonstrated that the investigated polyelectrolyte solutions have to be divided into four different concentration ranges (I–IV). In the dilute concentration range (range I) the buildup and decay of the electric birefringence proceed by a single process (τ_1). In this concentration range the interactions between the different molecules can be neglected, and the polyelectrolytes are present in a more or less stretched conformation. The birefringence in this concentration region is negative, and the molecules are oriented with their long axis in the direction of the electric field. The concentration range II starts at the concentration c_1* where the rotational volumes of the rods begin to overlap. A second effect (τ_2) with opposite sign of the first effect is present together with the τ_1 process. The time constant τ_2 of the second effect is longer than the time constant of the first effect. Its amplitude can also be larger than the amplitude of the first effect, and the total sign of the birefringence becomes positive. It is concluded that during this second process the macromolecules are oriented perpendicular to the electric field. At even higher concentrations (range III) a third effect (τ_3) with the same sign as the first effect becomes visible. This effect is likely due to the cooperative motion of an entangled transient network structure, which again can be oriented parallel to the electric field. In a very small concentration range the three processes can be observed simultaneously. At even higher concentrations the birefringence vanishes. This seems to be a consequence of the coiling of the macromolecules (range IV). The observed results on the polyelectrolytes are very similar to results that have been obtained previously on ionic surfactants that form rodlike micelles. The principal results on the two different systems are the same, but rodlike micelles possess an inherent stiffness in comparison to the investigated polyelectrolytes. The concentration-dependent flexibility of the polyelectrolytes causes some special features of the anomalous birefringence behavior. It can be concluded that all systems with charged anisometric particles show the anomaly of the electric birefringence.

Introduction

Polyelectrolytes represent a class of macromolecules that carry a large number of elementary charges distributed along the macromolecular chain. Many polyelectrolytes are stiff rodlike particles, e.g., tobacco mosaic virus (TMV) or DNA. In comparison to TMV, many layer silicates are also stiff but look like disks as, for example, saponite. Polyelectrolytes, however, can also be flexible, as is the case for most of the synthetic polyelectrolytes.

In the past two decades the theory for flexible polyelectrolytes has advanced considerably. It is generally accepted that in the absence of salt polyelectrolytes are more or less in the stretched conformation in dilute solutions. With increasing concentration interactions between the polyions become important and the polyelectrolytes are no longer independent from each other. As a consequence a rod to coil transition occurs if the polyelectrolytes do not possess an inherent stiffness.[1]

The interactions have a strong influence on the experimental results, and it is often not easy to interpret the results without making simplifying assumptions. Especially in scattering experiments many problems arise with increasing concentration for the interpretation of the data, and it is difficult to get unambiguous information from the results about the conformation of the macromolecules. In this paper we show that the electric birefringence method is a powerful tool to monitor the electrostatic interactions between the charged polyelectrolyte molecules. The electric birefringence signal contains detailed information from which the conformation of the polyelectrolyte molecules for different concentrations can be elucidated and different concentration ranges can be distinguished.

Polyelectrolytes can be aligned by applying an electric pulse (transient electric birefringence (TEB)) or an alternating electric field (dynamic electric birefringence (DEB)) to the solution. In dilute solutions the behavior is well understood. The anisotropy of the ionic polarizability is very strong in comparison to the electronic polarizability or the effect of a permanent dipole moment.[2] Therefore the polyelectrolytes can be easily oriented in the direction of the electric field, which results in a time-retarded buildup of the birefringence Δn until a stationary value Δn_{st} is reached. At the end of the pulse the birefringence decays with a characteristic time constant, from which it is possible to calculate a length of the polyelectrolytes. In the normal case the Δn_{st} value is also independent of the frequency in DEB measurements.

Deviations from that normal behavior occur at higher concentrations, as has been reported for biological polyelectrolytes,[3] bentonite dispersions,[4] V_2O_5 dispersions,[5] poly(tetrafluoroethylene) fibers (p-TFE),[6] and surfactant systems.[7] A second effect is usually observed that has opposite sign to that of the first one. This behavior has been generally called the anomaly of the electric birefringence. In extensive studies of surfactant systems it was shown that the anomaly occurs only with charged micelles in a certain concentration range.[8] In comparison to polyelectrolytes micelles offer many advantages. It is possible to charge a neutral, rodlike micelle by addition of small amounts of ionic surfactant to introduce the anomaly. Alternatively, it is possible to suppress the electrostatic interactions and the anomaly by addition of small amounts of salt. For charged micellar systems it was possible to distinguish clearly three different concentration ranges. In the first, dilute, region no interactions can be observed. In the second, semidilute, region the electric double layers

0024-9297/91/2224-0256$02.50/0

of the rods overlap, and it was concluded that the rods are oriented perpendicular to the electric field, because it seems to become easier to polarize the micelles perpendicular to the main axis than parallel. In the third, concentrated, region an entanglement network is formed from the rods, and the particles are again oriented in the normal way parallel to the electric field.

The aim of the present study is to compare the results of micellar systems with results of polyelectrolytes. For the polyelectrolytes we also hoped to obtain information about their conformation and flexibility. The chosen polyelectrolytes (poly(sodium *p*-styrenesulfonate)) have already been studied by several groups,[9,10] and an anomaly has also been found at certain concentrations. However, until now there does not exist a complete study and interpretation of the time and frequency behavior of this polyelectrolyte in the electric field over a large concentration range. The experimental results that have been obtained by different groups differ considerably. Sometimes an anomalous behavior was observed and sometimes not. Furthermore the experiments did not cover the whole concentration range, and the explanation of the data is not consistent with the results in other charged systems. Most of the measurements on polyelectrolytes deal with low molar mass salt containing solutions.[11]

We decided therefore to reinvestigate the behavior of polyelectrolytes in salt-free solutions. At the same time we were interested to learn how the molecular weight of the samples influenced the data, and for this reason we studied samples with different molecular weights. Finally, we intended to obtain results over a concentration range as wide as possible in order to be able to compare the results with the theory of polyelectrolytes that was developed by Odijk.

In 1979 Odijk[12] established a theory for polyelectrolytes based on the model of a wormlike chain. On the basis of this model at least four different concentration ranges have to be differentiated. It was therefore also of interest to us to find out whether the four theoretically predicted concentration ranges could be distinguished on the basis of the electric birefringence.

Experimental Section

Materials. As polyelectrolyte we have chosen poly(sodium *p*-styrenesulfonate) (NaPSS), because it was possible to obtain this polyelectrolyte with a very narrow molecular mass distribution of 1.06. Problems arising from polydispersity can therefore be neglected. Additionally, the high charge density of this polyelectrolyte is a further advantage, especially for studying electrostatic interactions. The poly(sodium *p*-styrenesulfonate) was a gift of BASF A.G., Ludwigshafen. BASF A.G. had obtained it from Chemical Standard Service, Mainz, and dialyzed it to remove low molar mass salt. Three different molar masses with M_w = 100 000 g/mol (NaPSS-100000), 400 000 g/mol (NaPSS-400000), and 1 200 000 g/mol (NaPSS-1200000) were available. These polyelectrolytes were used without further purification.

Electric Birefringence Instruments. The electric birefringence signals were measured at 25 °C and at a laser wavelength λ of 632.8 nm. The details of the TEB and DEB instruments have been well described.[13] In the TEB apparatus rectangular, high-voltage pulses of short rise and decay times (25 ns) were applied to the solutions. In all measurements the pulses were long enough to reach the steady-state value Δn_{st} of the electric birefringence. The time constant of the decay and the amplitude of the stationary value were measured.

For highly viscous solutions and for very small birefringence values it was necessary to use sinusoidal pulses with varying frequencies in the DEB apparatus. The frequency of the ac field covered a range from 10 Hz to 100 kHz. In addition to the stationary amplitude and the time constant of the decay, the alternating amplitude was recorded. To determine the sign of the birefringence a quarter-wave device was introduced between analyzer and cell. A lock-in amplifier was used to detect the small birefringence values for measurements at low electric fields.

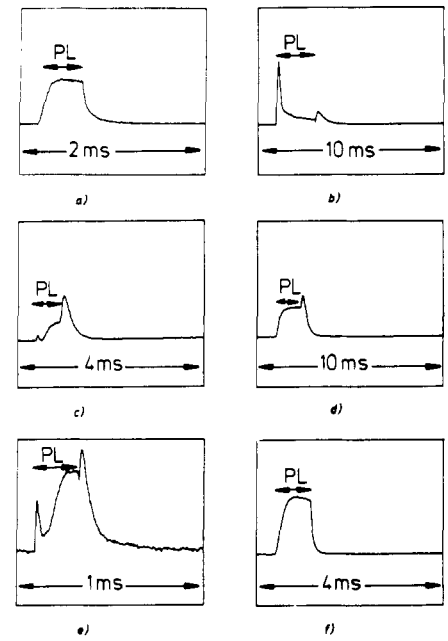

Figure 1. Change of the TEB signals with increasing NaPSS-400000 concentration. PL = electric pulse length, T = 25 °C, $E = 7.5 \times 10^4$ V/m. (a) c = 0.01 g/L, $\Delta n_{st} = -1.6 \times 10^{-8}$; (b) c = 0.1 g/L, $\Delta n_{st} = -3.4 \times 10^{-8}$; (c) c = 0.3 g/L, $\Delta n_{st} = +5.4 \times 10^{-8}$; (d) c = 1 g/L, $\Delta n_{st} = +16.8 \times 10^{-8}$; (e) c = 4 g/L, $\Delta n_{st} = -1.65 \times 10^{-8}$; (f) c = 10 g/L, $\Delta n_{st} = -14.8 \times 10^{-8}$.

Results

The behavior of poly(sodium *p*-styrenesulfonate) in the electric field depends on different factors. One of them is the concentration, and we show that at least three distinct concentration ranges can be distinguished. The main features of the poly(sodium *p*-styrenesulfonate) are explained on the sample with a molecular weight of 400 000. However, the results are then compared with the higher and the lower molecular weight samples.

In dilute solutions without interactions the behavior of the polyelectrolyte is normal and corresponds with the expected behavior of charged rodlike micellar systems or stiff biological molecules. Figure 1a shows a TEB signal of a 0.01 g/L solution. At the beginning of the electric pulse the polyelectrolytes are oriented in the electric field, and the birefringence increases up to a stationary value Δn_{st}. At the end of the pulse the birefringence decays with the time constant τ_1. Rise and decay curves are nearly symmetrical. With increasing concentration a second effect with opposite sign is observed, and the birefringence signal exhibits the anomalous behavior (Figure 1b). The birefringence Δn increases similarly as in the dilute region (first effect), but then a maximum is reached and Δn decreases again with a slower time constant until again a stationary value is reached (second effect). Switching off the pulse leads to a relaxation of the first process. Therefore the birefringence Δn decreases, passes through zero, and then increases again until also the second opposite effect relaxes to zero with the time constant τ_2. The sign of the first process corresponds to a negative birefringence, while the second process is positive.

With increasing concentration the second effect becomes stronger than the first effect (Figure 1c). Hence the birefringence Δn passes through zero and Δn_{st} becomes

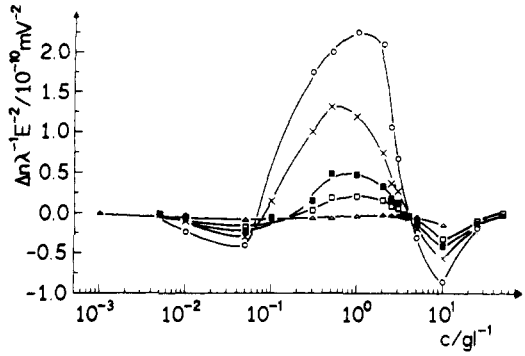

Figure 2. $\Delta n_{st}\lambda^{-1}E^{-2}$ values as a function of the NaPSS-400000 concentration at different field strengths. $T = 25$ °C. (○) $E = 2.5 \times 10^4$ V/m; (×) $E = 5.0 \times 10^4$ V/m; (■) $E = 7.5 \times 10^4$ V/m; (□) $E = 1.0 \times 10^5$ V/m; (△) $E = 2.0 \times 10^5$ V/m.

positive. At the end of the pulse Δn increases because the negative effect relaxes first and the second effect becomes stronger. Δn reaches a maximum and relaxes with the time constant τ_2. With a further increase of concentration the second effect becomes even larger, and in Figure 1d at 1 g/L the first effect can only be recognized in the decay curve. At 4 g/L the signal has totally changed (Figure 1e). First Δn rises to a maximum (first effect), then decreases to a minimum (second effect), and rises again until Δn_{st} is reached. The third effect has again a negative sign. Switching off the pulse results in a small dip, which is due to the first relaxation time τ_1. Then the second effect relaxes with τ_2 and Δn increases again to a maximum. Finally, also the third effect relaxes (τ_3) and Δn reaches zero. These three effects can only be observed simultaneously in a very small concentration range. At higher concentrations the third effect dominates, and the behavior seems normal again as demonstrated in Figure 1f for 10 g/L.

The Δn_{st} values not only depend on the concentration but also on the field strength E. If the Kerr law is valid, Δn_{st} should be proportional to E^2, and it is possible to calculate a Kerr constant B:

$$B = \Delta n_{st}/\lambda E^2 \quad (1)$$

In Figure 2 the $\Delta n_{st}/\lambda E^2$ values are plotted as a function of the concentration. The deviations of the Kerr law are obvious, because the $\Delta n_{st}/\lambda E^2$ are not constant for the different field strengths. A subdivision into the three concentration ranges can be recognized. In the dilute region up to $c = 0.05$ g/L and in the concentrated region above 3.5 g/L the birefringence is always negative, while in the anomaly range between $c = 0.05$ and 3.5 g/L the sign is positive at low field strengths and may become negative at high field strengths. This can also be seen in Figure 3, where the TEB signals of a 0.1 g/L solution are plotted for four different field strengths. In Figure 3a Δn_{st} is positive and the first effect is small in comparison to the second effect. The increasing field strength in Figure 3b strengthens the first effect, and Δn_{st} becomes smaller. This is continued in Figure 3c, where the first effect is now larger than the second one and Δn_{st} reaches only a negative value. With further increasing field strength the first effect becomes much stronger than the second one (Figure 3d). Hence the increasing electric field favors the first effect more than the second effect. This is also demonstrated in Figure 4, where the birefringence is separated into the two effects. The part of the birefringence that is due to the first effect is designated as $\Delta n_1(-)$, while the second effect is marked as $\Delta n_2(+)$. The second effect reaches a saturation value at high field strength, while the first effect

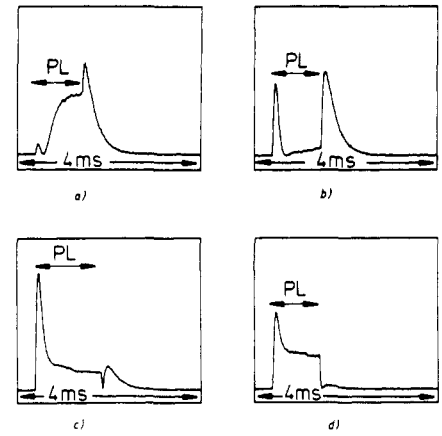

Figure 3. TEB signals of $c = 0.1$ g/L NaPSS-400000 at different field strengths. $T = 25$ °C. (a) $E = 2.5 \times 10^4$ V/m, $\Delta n_{st} = +2.55 \times 10^{-8}$; (b) $E = 5.0 \times 10^4$ V/m, $\Delta n_{st} = +1.40 \times 10^{-8}$; (c) $E = 7.5 \times 10^4$ V/m, $\Delta n_{st} = -3.43 \times 10^{-8}$; (d) $E = 1.0 \times 10^5$ V/m, $\Delta n_{st} = -8.77 \times 10^{-8}$.

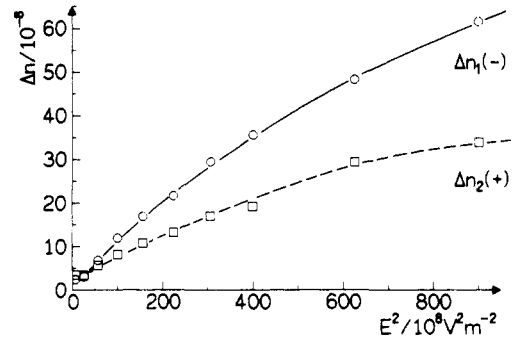

Figure 4. Separation of the birefringence into the first effect $\Delta n_1(-)$ and the second effect $\Delta n_2(+)$ as a function of E^2. $c = 0.1$ g/L NaPSS-400000, $T = 25$ °C.

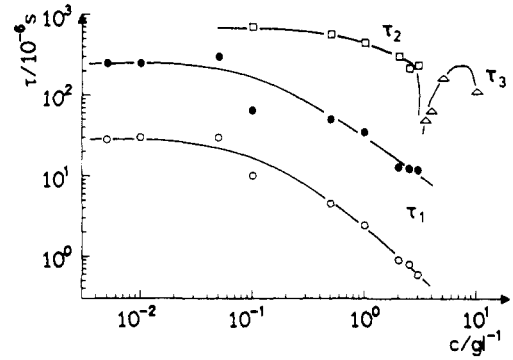

Figure 5. The three relaxation times τ_1, τ_2, and τ_3 of NaPSS-400000 as a function of the concentration. The relaxation process τ_1 has to be fitted with two time constants. $T = 25$ °C.

increases further on.

In Figure 5 the above-mentioned three relaxation times τ_1, τ_2, and τ_3 are plotted as a function of the concentration. The time constants τ_2 and τ_3 correspond to monoexponential decays, while the shortest relaxation process has to be fitted with two exponential functions, and hence two different time constants are plotted in Figure 5 for τ_1. It would probably also be possible to fit the data with a stretched exponential as has recently been done by Degiorgio et al.[14] We have used two exponential functions and assumed that the two time constants correspond to the extreme states of the polyelectrolyte that can undergo coiling. The coiling effects a size distribution of the end-to-end distance. Hence the longer time constant for τ_1 can be attributed to polyelectrolytes, which are in a stretched

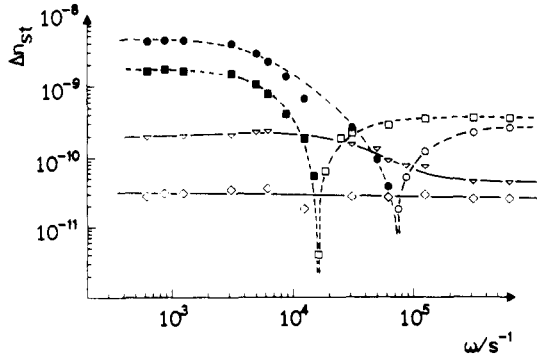

Figure 6. Stationary birefringence Δn_{st} in DEB measurements as a function of the frequency ω for different concentrations. The filled symbols represent a positive birefringence, while the empty symbols stand for negative birefringence. $T = 25$ °C, $E = 2.9 \times 10^3$ V/m. (◇) 0.01 g/L NaPSS-400000; (□) 0.1 g/L NaPSS-400000; (○) 1.0 g/L NaPSS-400000; (▽) 10 g/L NaPSS-400000.

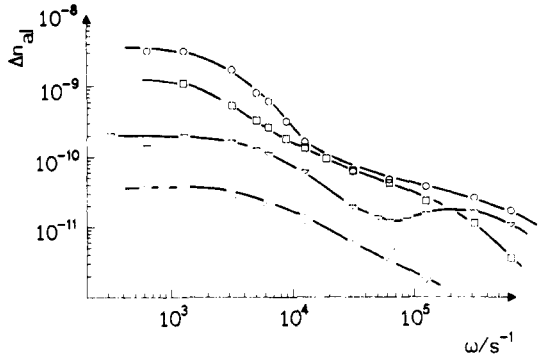

Figure 7. Alternating birefringence Δn_{al} in DEB measurements as a function of the frequency ω for different concentrations. $T = 25$ °C, $E = 2.9 \times 10^3$ V/m. (◇) 0.01 g/L NaPSS-400000; (□) 0.1 g/L NaPSS-400000; (○) 1.0 g/L NaPSS-400000; (▽) 10 g/L NaPSS-400000.

conformation. For a comparison of the data the longer time constant of τ_1 has always been taken. The relaxation time τ_1 remains constant up to $c = 0.05$ g/L and then decreases. The relaxation time τ_2 becomes also shorter with increasing concentration, while τ_3 passes through a maximum. However, τ_3 is always larger than τ_2 as can also be seen in Figure 1f.

TEB measurements yield the time-dependent behavior of the particles. With DEB measurements with sinusoidal fields it is also possible to measure the frequency-dependent behavior, which contains the same information as the TEB signals. In Figure 6 the stationary part Δn_{st} of the birefringence is plotted for different concentrations as a function of the frequency ω. In the dilute region no frequency dependence is visible as is demonstrated for $c = 0.01$ g/L, and Δn_{st} is always negative. This behavior is typical for a pure induced dipole moment. At a concentration of $c = 0.1$ g/L the anomalous region is reached. At high frequencies Δn_{st} is negative and corresponds with the dilute region and a quick induced dipole. With decreasing frequency the birefringence becomes smaller, passes through zero at $\omega = 17\,000$ s^{-1}, and increases again at lower frequencies. However, the sign of the birefringence has changed to positive. At very low frequencies Δn_{st} achieves a constant value. At a concentration of 1 g/L the anomaly is extended and the zero pass is shifted to $\omega = 68\,000$ s^{-1}. In the third region at a concentration of 10 g/L Δn_{st} is negative again at all frequencies, but a clear step between the low and the high frequencies is visible. Hence the behavior at low frequencies corresponds with Δn_{st} of the TEB measurements, and the frequency is low enough to activate also the second and third effects, while at high frequencies only the first, always negative, effect is activated. A comparison of the Δn_{st} values at high frequencies shows an increase of Δn_{st} from $c = 0.01$ to $c = 0.1$ g/L. This is due to the concentration increase, while the macroions are still very stretched. At $c = 1$ g/L the effect of the concentration increase is overcompensated by the coiling of the macroions. Hence the optical polarizability becomes smaller and Δn_{st} decreases again.

In DEB experiments the stationary birefringence is superimposed by an alternating birefringence Δn_{al}, which is plotted in Figure 7 for the same concentrations as in Figure 6 as a function of the frequency ω. The behavior at concentrations smaller than 0.1 g/L is typical for an induced dipole moment. Therefore the values for Δn_{al} at a concentration of 0.01 g/L NaPSS-400000 are constant up to a certain frequency until they decrease to zero at

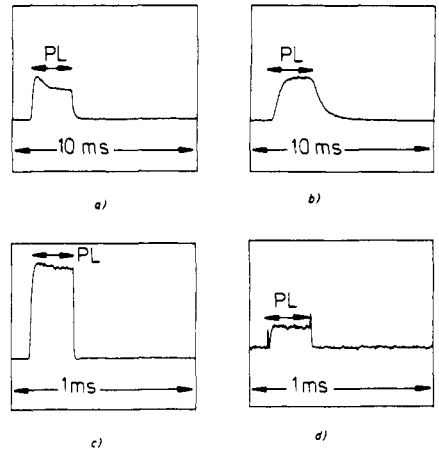

Figure 8. TEB signals of the NaPSS-1200000 and NaPSS-100000 samples. $E = 7.5 \times 10^4$ V/m, $T = 25$ °C. (a) NaPSS-1200000, 0.01 g/L, $\Delta n_{st} = -3.1 \times 10^{-8}$; (b) NaPSS-1200000, 2.0 g/L, $\Delta n_{st} = -8.4 \times 10^{-8}$; (c) NaPSS-100000, 1.0 g/L, $\Delta n_{st} = -3.4 \times 10^{-8}$; (d) NaPSS-100000, 5.0 g/L, $\Delta n_{st} = +0.9 \times 10^{-8}$.

higher frequencies. For the other concentrations the behavior corresponds only at high frequencies to such an induced dipole moment. With decreasing frequencies different steps are visible, which belong to the activation of the second (0.1 and 1 g/L) and third effect (10 g/L). At very low frequencies Δn_{al} and Δn_{st} accept the same values.

The anomaly can also be observed on the samples with molecular weights of 1 200 000 and 100 000, but there are some differences to be mentioned. In Figure 8a the 1 200 000 sample shows already at a concentration of 0.01 g/L a weak second effect, while at $c = 2$ g/L the third effect dominates (Figure 8b). Hence the anomalous region is shifted to lower concentrations in comparison to the 400 000 sample. In contrast to that the 100 000 sample shows the anomaly not before 1 g/L (Figure 8c), and at $C = 5$ g/L the second, positive, effect is stronger than the first one (Figure 8d). A third effect can no longer be found, and the birefringence vanishes completely at a concentration of 20 g/L. Therefore the anomaly region is displaced to higher concentrations.

An increase of the temperature does not effect a strong change in the anomaly region as demonstrated in Figure 9 for a sample of 0.1 g/L NaPSS-400000. The characteristic features of the two signals at 5 and 50 °C are the same. Only the absolute values of the birefringence decrease, and the time constants τ_1 and τ_2 become shorter with increasing temperature (Figure 10). This is a consequence of the decreasing solvent viscosity and the intensified Brownian

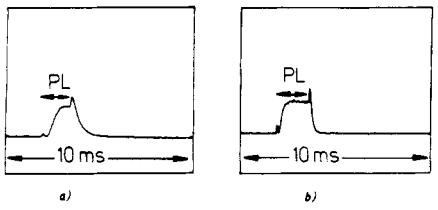

Figure 9. TEB signals of NaPSS-400000 at two different temperatures. c = 0.1 g/L, $E = 2.5 \times 10^4$ V/m. (a) T = 5 °C, $\Delta n_{st} = +3.1 \times 10^{-8}$; (b) T = 50 °C, $\Delta n_{st} = +1.8 \times 10^{-8}$.

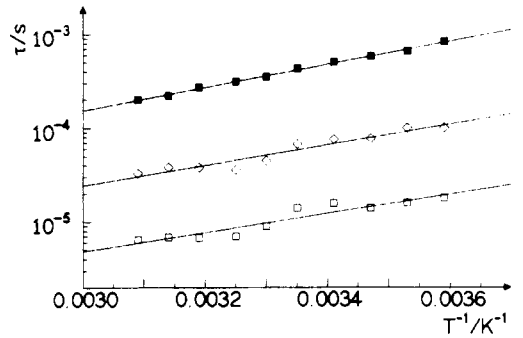

Figure 10. Time constants τ_1 and τ_2 of NaPSS-400000 at different temperatures. The relaxation process τ_1 has to be fitted with two time constants. (□, ◇) τ_1; (■) τ_2.

molecular motion. Within experimental accuracy the size of the polyelectrolytes is not changed with increasing temperature, and the interactions also remained constant, in spite of the increasing Debye screening length.

Discussion

Qualitatively, we find the same behavior of polyelectrolytes in the electric field as for charged rodlike micellar systems. With increasing concentration the sign of the birefringence signal changes from negative to positive and back to negative again before it vanishes altogether. These changes in sign can be assigned to three different processes. The fastest process τ_1 is due to the free rotation of the polyelectrolyte chain. The negative birefringence corresponds to an orientation parallel to the electric field, which is as expected for rods containing aromatic rings. Polyelectrolytes possess a higher flexibility than ionic micellar rods, which depends furthermore on the concentration and the molecular weight. This is probably the reason why it is not possible to fit the fast relaxation process of NaPPS-400000 and NaPSS-1200000 with only a single time constant τ_1. As is visible in Figure 4 the τ_1 values remain constant up to 0.05 g/L. In contrast to the higher molecular weight samples the NaPSS-100000 sample could be fitted with only one time constant. This is probably due to the relative stiffness of the small molecule in comparison to the other very long samples. At a certain concentration the τ_1 values for all three samples become shorter and the anomaly appears. In contrast to that, charged micellar rods are always stiffer but can change their size depending on the concentration and the interactions. As polyelectrolytes are naturally of constant size, they decrease the interactions by coiling. However, this is only possible to a certain degree, because the neighboring charges try to stretch the molecule. Hence an energetically preferred conformation between completely stretched rod and Gaussian coil is achieved. According to the theory of Peterlin and Stuart,[15] the relaxation time τ_1 is directly related to a rotational diffusion coefficient D_r:

$$D_r = 1/(6\tau_1) \quad (2)$$

If it was necessary to use two time constants for the relaxation process τ_1 the longer time constant was always taken to calculate D_r. D_r is related to a particle length L according to an equation of Newman:[16]

$$D_r = \frac{3kT}{\pi\eta L^3}[\ln p - 0.76 + 7.5[1/\ln(2p) - 0.27]^2] \quad (3)$$

where kT is thermal energy, η is solvent viscosity, and p is the axial ratio.

The diameter R of the rods was assumed to be 10 Å and is not critical because the result is fairly insensitive to this value. It should be mentioned that eq 3 is only valid for stiff particles; nevertheless, it is used for a comparison of the data.

Table I
Mean Distance $\langle r \rangle$, Length L, and Relaxation Time τ_1 for Different NaPSS-400000 Concentrations

c, g L^{-1}	$\langle r \rangle$, Å	L, Å	τ_1, 10^{-6} s
0.001	8724		
0.005	5102	3237	250 ± 28
0.01	4049	3237	250 ± 30
0.05	2368	3455	300 ± 30
0.1	1879	1995	65 ± 10
0.5	1100	1815	50 ± 4.5
1.0	872	1595	35 ± 2.4
2.0	692	1113	13 ± 0.9
2.5	642	1097	12 ± 0.8
3.0	605	1081	12 ± 0.6

The anomaly of the electric birefringence appears first at the overlap concentration of the diffuse double layers. In Table I the mean distances $\langle r \rangle$ between the macromolecules at different NaPSS-400000 concentrations are listed. $\langle r \rangle$ is given by

$$\langle r \rangle = (cN_L/M)^{-1/3} \quad (4)$$

where c is the polyelectrolyte concentration in g/L, N_L is Avogadro's constant, and M is the molecular weight.

A comparison of the contour length l (4850 Å) with the calculated values L in Table I shows that already at very low concentrations the L values are smaller than the completely stretched macromolecule. With increasing concentration L becomes smaller and the macromolecule is more and more coiled to reduce the interactions. At a concentration c_1* of 0.05 g/L the mean distance $\langle r \rangle$ becomes smaller than L. Hence the rods overlap and it is difficult to polarize the rods along their main axis in the direction of the electric field. The counterions that are displaced from one rod are supplemented by an overlapping neighboring rod. As was assumed for micellar systems,[8] it is likely, however, that the counterions can still be displaced perpendicular to the main particle axis. This displacement of the counterions must therefore lead to a buildup of a dipole moment perpendicular to the axis of the polyelectrolyte, and the macromolecules are partly oriented perpendicular to the electric field. Therefore a positive birefringence results, which can overcompensate the negative birefringence of the particles oriented in the direction of the field.

While at present we cannot unambiguously prove the perpendicular orientation to the electric field, we nevertheless have much confidence in this interpretation. Some experimental results on other charged rodlike systems do indeed show that charged rods can orient perpendicular to electric fields.

A confirmation of the perpendicular-oriented rods comes from the results of dichroism measurements of Yamaoka and Matsuda,[10] who observed a field-strength-dependent change of the sign at a certain concentration of NaPSS. Also neutron scattering experiments of Hoffmann et al. for p-TFE fibers[17] show in the anomaly region a frequency-

Table II
Mean Distance $\langle r \rangle$, Length L, and Relaxation Time τ_1 for Different NaPPS-100000 Concentrations

c, g L^{-1}	$\langle r \rangle$, Å	L, Å	τ_1, 10^{-6} s
0.05	1492	784	5.3
0.1	1182	766	4.7
0.2	939	754	4.5
0.5	692	760	4.6
1.0	549	853	6.3 ± 0.5
3.0	381	649	3.0 ± 0.3

dependent rotation of the correlation peaks, which can only be interpreted in terms of a perpendicular orientation of the fibers in the electric field. A further confirmation comes from the light scattering results of the p-TFE fibers perpendicular and parallel to an applied electric field, which also depends on the frequency.[6]

From scattering experiments on NaPSS solutions it is well-known that even in dilute solutions a maximum of the scattering intensity appears as a function of the scattering vector q.[18] This so-called correlation peak is an indication for an ordered structure due to long-range interactions. In the semidilute concentration range the overlapping rods have minimized their energy. By the perpendicular rotation of the rods this order is destroyed, and only in a coupled rotational–translational motion is it possible to reach again an energetically preferred distribution. Hence the relaxation time τ_2 has to be somewhat longer than τ_1 to reach again an energetically preferred situation.

With further increasing concentration this anomalous behavior is overcome by a third effect at a certain concentration c_2^*. At this concentration the τ_2 process vanishes rather abruptly and is no longer observable. It is conceivable that the τ_2 process disappears when the electric double layers of the rods begin to overlap also perpendicular to the main axis. Above the concentration c_2^* a three-dimensional network is likely to be present, which can also be oriented in the electric field. As the sign of the third effect is the same as the first one and opposite to the second one, it seems probable that the polyelectrolyte chains are oriented in the direction of the electric field. Although the real structure of the network is unknown, it can be expected that it is built up by entangled macroions possessing an anisometric structure. Hence in a small concentration range a transition from the overlapping macroions to a three-dimensional structure occurs. This structure may also be regarded to consist of domains of strongly correlated macroions. In this concentration range the rods become more flexible and more coiled. Hence the birefringence vanishes completely at a certain concentration c_3^*. Above c_3^* the macromolecules are more or less coiled, and no birefringence can be observed. This is in correspondence with birefringence results on uncharged polymers such as polystyrene, which only exhibit a small birefringence due to the monomer units.[19] As the ionic strength is well above c_3^*, only small field strengths can be used, and small birefringences are no longer detectable.

Most of the measurements were obtained on the samples with a molecular weight of 400 000. The results clearly reveal four distinct concentration regions. For samples with molecular weights of 100 000 and 1 200 000 fewer results were obtained. Some of the results are given in Tables II and III. Since the molecular weights of the samples are different, we can expect that the different concentration regions for these systems are shifted with respect to the same concentration regions of the sample with a molecular weight of 400 000. Qualitatively, this seems to be the case. There are, however, marked differences in the behavior of the three samples, and the four concentration regions are not so clearly expressed in the results of the other systems.

Table III
Mean Distance $\langle r \rangle$, Length L, and Relaxation Time τ_1 for Different NaPSS-1200000 Concentrations

c, g L^{-1}	$\langle r \rangle$, Å	L, Å	τ_1, 10^{-6} s
0.005	7358	3454	300 ± 30
0.01	5840	3237	250 ± 26
0.05	3415	3574	330 ± 30
0.1	2710	3574	330 ± 20
0.2	2151	3141	230 ± 14

The differences of the results are probably due to the fact that the ratio of the persistence length to the contour length is very much different in the three samples. This is most obvious when we compare the largest relaxation times in the dilute case. For NaPSS-100000 and -400000 we find τ_1 values that correspond to a length scale of two-thirds of the completely stretched chain in the all-trans conformation. It is unlikely, however, that the polyelectrolytes are present in the all-trans conformation, because in this mode the charges of the sulfonate groups would be relatively close to each other and the interaction energy would be large. To minimize this interaction energy and to distribute the charge density evenly along the backbone necessitate the formation of rotamers. Such a chain would be considerably shorter than a completely all-trans chain. For NaPSS-100000 and 400000 the chains seem to be in this state. This means that the persistence length of NaPSS-400000 has still about the same length as this conformation. It furthermore seems that NaPSS-100000 in the dilute state has a much longer persistence length than the polyelectrolyte in its equilibrium condition. For this reason all the chains have the same length, and single-exponential behavior is observed in the decay curves. For NaPSS-400000 the persistence length seems to be equal to the length of the polyelectrolyte in its equilibrium situation. This results in a distribution of the end-to-end distance and multiexponential decay.

For NaPSS-1200000 finally the observed relaxation times τ_1 are about the same as for NaPSS-400000. The end-to-end distance of the chains and hence the dimensions of the NaPSS-1200000 coils are probably about the same as the length of NaPSS-400000. On the basis of these differences we can also qualitatively discuss other differences for the three systems. For NaPSS-100000 we observe with increasing concentration the range II with the two opposite effects and the anomalous behavior. As expected the concentration c_1^* is shifted upward with respect to NaPSS-400000. It is likely that the concentration c_2^* is also shifted upward. However, it was not possible to detect the τ_3 process. The birefringence signal vanishes in the concentration range II. It is conceivable that the concentration c_3^* does not depend on the molecular weight but only on the ionic strength of the solutions. For this system we reach coiling before the appearance of the τ_3 process.

As already mentioned the persistence length of NaPSS-1200000 is much shorter than the contour length. In spite of this the critical concentrations c_1^* and c_2^* are shifted to lower concentrations in comparison with NaPSS-400000. For the largest molecular weight sample the concentration c_3^* was not measured, but it can be assumed that it is around the same concentration as c_3^* for NaPSS-400000.

Two effects seem to be responsible for the behavior of the polyelectrolytes in the electric field. With increasing

Table IV
Comparison of the Critical Concentrations of the Odijk Theory ($c_{p,g}$, c_p^*, c_p^{**}) with the Critical Concentrations (c_1^*, c_2^*, c_3^*) from the Electric Birefringence Results[a]

M_w	$c_{p,g}$	c_p^*	c_p^{**}	c_1^*	c_2^*	c_3^*
100 000	9.3×10^{-2}	0.314	8.24	1		20
400 000	5.8×10^{-3}	0.078	8.24	0.05	3.5	50
1200 000	6.4×10^{-4}	0.026	8.24	0.01	1.0	

[a] Concentrations in g L^{-1}.

concentration, molecular weight determines when the polyelectrolytes begin to coil. The higher the molecular weight, the later the coiling occurs. At the same time the interactions depend on the size of the rods. Small rods show the interactions at higher concentrations than large rods. This is in agreement with the results on micellar systems, where it could be shown that the anomaly region is shifted to lower concentrations with increasing rod length. However, in contrast to polyelectrolytes, micellar systems are very stiff and do not coil. Therefore the anomaly region of micellar systems is very small in comparison to polyelectrolytes, where the interactions are reduced by the coiling. Hence there should also exist a lower limit for the molecular weight up to which no anomaly appears. This can already be seen for the NaPSS-100000, for which c_2^* vanishes.

Using the model of the wormlike chain, Odijk[12] derived a theory with which he was able to define different concentration ranges for polyelectrolytes in the absence of excess salt. According to this theory, the persistence length L_e is given for NaPSS by the equation

$$L_e = (16\pi Q A c_m N_L)^{-1} \quad (5)$$

Q denotes the Bjerrum length (7.14 Å in H_2O at 25 °C), A is the distance between two charges on the macromolecule, and c_m is the concentration in monomeric moles per unit volume. In the very dilute concentration range the macromolecule is therefore completely stretched until at a concentration of $c_{p,g}$ some local ordering appears:

$$c_{p,g} = (Al^2 N_L)^{-1} \quad (6)$$

The concentration c_p^*, at which L_e is equal to the contour length l, is a yardstick for another concentration regime above which the macromolecule is characterized by an increased flexibility:[12,20]

$$c_p^* = (16\pi Q A l N_L)^{-1} \quad (7)$$

At a further concentration c_p^{**} that should be independent of the molecular weight the lattice melts:

$$c_p^{**} = 0.4(4\pi Q_2 A N_L)^{-1} \quad (8)$$

In Table IV the values for the critical concentrations are listed and compared with the critical concentrations defined by the electric birefringence. A concentration $c_{p,g}$ cannot be detected with the electric birefringence. Instead it seems that the interactions can be neglected up to the concentration c_1^*. The macromolecules seem not to be completely stretched but seem to possess a constant size up to c_1^*, and only above c_1^* do the rods begin to coil. The concentration c_1^* is not a sharp point, and hence c_1^* has to be taken with caution. However, a comparison of c_1^* and c_p^*, especially for the higher molecular weight samples, shows a reasonable agreement. Hence the concentration region between c_1^* and c_2^* has to be considered as the overlap concentration of the polyelectrolytes but without network properties. At the concentration c_2^* a third relaxation process appears which seems to be due to a network. In micellar systems the time constant τ_3 is always longer than τ_2, but for polyelectrolytes the coiling of the rods causes a comparably low τ_3. This concentration c_2^* can be compared with c_p^{**}, which should be independent of the molecular weight. However, this is not the case; the transition concentration c_2^* occurs in a narrow region and depends on the size of the macromolecules. With further increasing concentration the time constant τ_3 becomes shorter and the amplitude vanishes at a certain concentration c_3^*. Hence at very high concentrations a further concentration region can be defined, where the solutions behave similar to normal polymer solutions.

Conclusions

The electric birefringence method is a very useful tool for elucidating the conformation of polyelectrolytes in solution. The results from the TEB or DEB experiments render detailed information about the conformation of the polyelectrolytes in the different concentration ranges, which can be distinguished. In the dilute region the polyelectrolytes are very extended, and interactions between the macromolecules can be neglected. However, only up to a certain length the NaPSS polyelectrolytes can be considered as completely stretched. At the overlap concentration of the rods electrostatic interactions increase very strongly, and the anomalous behavior appears between the overlap concentration c_1^* and the second critical concentration c_2^* at which a transient network is formed. In contrast to micellar systems the anomaly is extended over a larger area. This seems to be due to the increasing flexibility of the rods, which try to reduce the interactions. Hence at a certain concentration c_3^* the macromolecules are completely coiled, and birefringence can no longer be detected.

A comparison of the Odijk theory with the results of the electric birefringence shows some similarities, but the theory is not able to describe quantitatively the whole behavior of the polyelectrolytes. Nevertheless, the subdivision in different concentration ranges is in good agreement with the experimental results, but there does not exist a quantitative theory up to now that can describe the behavior at all concentrations.

The introduced critical concentrations c_1^*, c_2^*, and c_3^* are useful in comparing samples with different molecular weights. An increase of the molecular weight causes a shift of c_1^*, c_2^*, and c_3^* to lower concentrations. Below a certain molecular weight the critical concentration c_2^* vanishes and the polyelectrolytes are completely coiled. Therefore the anomaly can only be expected above a certain molecular length.

References and Notes

(1) Mandel, M. In *Encyclopedia of Polymer Science and Engineering*; John Wiley & Sons: New York, 1986; Vol. 11, p 739. Tsvetkov, V. N.; Andreeva, L. N. *Adv. Polym. Sci.* **1981**, *39*, 95.
(2) O'Konski, C. T. *J. Phys. Chem.* **1990**, *64*, 605. Mandel, M. In *Molecular Electro-Optics*; Krause, S., Ed.; Plenum Publishing Corp.: New York, 1983.
(3) Laufer, M. A. *J. Am. Chem. Soc.* **1939**, *61*, 2412.
(4) Mueller, H.; Sackmann, B. W. *Phys. Rev.* **1939**, *56*, 615. Mueller, H. *Phys. Rev.* **1939**, *55*, 792. Mueller, H. *Phys. Rev.* **1939**, *55*, 508. Norton, F. J. *Phys. Rev.* **1939**, *55*, 668. Shah, N. J.; Tompson, D. C.; Hart, C. N. *J. Phys. Chem.* **1963**, *67*, 1170.
(5) Errara, J.; Overbeck, J. T.; Sack, H. *J. Chem. Phys.* **1935**, *32*, 681.
(6) Angel, M.; Hoffmann, H.; Huber, G.; Rehage, H. *Ber. Bunsen-Ges. Phys. Chem.* **1988**, *92*, 10.
(7) Angel, M. Thesis, Bayreuth, 1985. Angel, M.; Hoffmann, H.; Krämer, U.; Thurn, H. *Ber. Bunsen-Ges. Phys. Chem.* **1989**, *93*, 184.
(8) Hoffmann, H.; Krämer, U.; Thurn, H. *J. Phys. Chem.* **1990**, *94*, 2027.

(9) Oppermann, W. *Makromol. Chem.* **1988**, *189*, 927. Oppermann, W. *Makromol. Chem.* **1988**, *189*, 2125. Tricot, M.; Housier, C. *Macromolecules* **1982**, *15*, 854.
(10) Yamaoka, K.; Matsuda, K. *J. Phys. Chem.* **1985**, *89*, 2779.
(11) Wijmenga, S. S.; van der Touw, F.; Mandel, M. *Macromolecules* **1986**, *19*, 1760. Wijmenga, S. S., van der Touw, F.; Mandel, M. *Polym. Commun.* **1985**, *26*, 172. Wijmenga, S. S.; Mandel, M. *J. Chem. Soc., Faraday Trans. 1* **1988**, *84*, 2483.
(12) Odijk, T. *Macromolecules* **1979**, *12*, 688. Odijk, T. *J. Polym. Sci., Polym. Phys. Ed.* **1979**, *15*, 477.
(13) Schorr, W.; Hoffmann, H. *J. Phys. Chem.* **1981**, *85*, 3160. Fredericq, E.; Houssier, C. *Electric Dichroism and Electric Birefringence*; Clarendon Press: Oxford, 1973.
(14) Bellini, T., Mantegazza, F.; Piazza, R.; Degiorgio, V. *Europhys. Lett.* **1989**, *10* (5), 499.
(15) Peterlin, A.; Stuart, H. A. *Hand- und Jahrbuch der chemischen Physik*; Eucken, A., Wolf, K. L., Eds.; Akademische Verlagsgesellschaft Becker D Erler Kom. Ges.: Leipzig, 1943; Bd. 8, p 44. Peterlin, A.; Stuart, H. A. *Z. Phys.* **1939**, *112*, 129.
(16) Newman, J.; Swinney, H. L.; Day, L. A. *J. Mol. Biol.* **1977**, *116*, 593.
(17) Angel, S.; Hoffmann, H. Poster at the Bayreuth Polymer Symposium, Bayreuth, 1989.
(18) Ise, N.; Okubo, T.; Kunugi, S.; Matsuoka, H.; Yamamoto, K.; Ishii, Y. *J. Chem. Phys.* **1984**, *81*, 3294.
(19) Champignon, J. V.; Meeten, G. H.; Southwell, G. W. *Polymer* **1976**, *17*, 651.
(20) Skolnick, J.; Fixman, M. *Macromolecules* **1977**, *10*, 944.

Registry No. NaPSS, 25704-18-1.